

Evaluation of Low- and Intermediate-Temperature Cracking Performance of Fiber-Reinforced Asphalt Mixtures

Transportation Research Record
1–13© National Academy of Sciences:
Transportation Research Board 2023
Article reuse guidelines:sagepub.com/journals-permissions

DOI: 10.1177/03611981231211900

journals.sagepub.com/home/trr

Ali Raza Khan¹, Ayman Ali¹ , Yusuf Mehta^{1,2} ,
and Mohamed Elshaer³

Abstract

This study was conducted to assess the impact of aramid fiber reinforcement on the fatigue and thermal cracking performance of asphalt mixtures at intermediate and low temperatures, respectively. The study also involved evaluating the experimental consistency and ranking fiber-reinforced asphalt mixtures (FRAMs) based on their performance. One aggregate (diabase stone), one binder type (PG 76-22), and two combinations of aramid fibers, added at different dosages, were used to produce three FRAMs. These fibers included polyolefin/aramid (PFA) fibers at 0.05% dosage by mix weight and Sasobit-coated aramid (SCA) fibers at 0.01% and 0.02% dosages. An unreinforced (control) mix was also produced without any reinforcement. All mixtures were produced at a batch plant by keeping their binder content constant (at 5.5%). The manufacturer recommended dry and wet mixing times were used for better fiber distribution and represent actual mixing conditions. The laboratory performance of plant-produced FRAMs was assessed to characterize the low- and intermediate-temperature cracking performance. The indirect tension asphalt cracking test, semi-circular bend test, three-point bending beam tests, and uniaxial fatigue tests were performed at intermediate temperature; the disk shape compact tension test and thermal stress restrained specimen test tests were performed at low temperature. Fibers were successful at improving the fatigue cracking of asphalt mixtures based on intermediate-temperature testing results. In addition, fiber reinforcement, regardless of dosage and combination, showed improvements in low-temperature (thermal) cracking performance. Furthermore, based on ranking analysis for selected performance indicators from each experiment, the SCA 0.02% reinforced mix on average showed the highest cracking resistance.

Keywords

asphalt materials, selection and mix design, fibers for asphalt, infrastructure, materials

Asphalt concrete (AC) is susceptible to fatigue and thermal cracking. Typically, fatigue and thermal cracking failures of AC are dominant phenomena at intermediate and low temperatures. Fatigue cracking is load-associated failure and thermal cracking is non-load associated. Fatigue cracks are caused by repeated heavy traffic and originate either from top or bottom of the AC layer and propagate in the opposite direction. In comparison, thermal cracking is a major issue in cold regions since it causes brittleness in AC (at cold temperatures), which in turn prevents the dissipation of thermal stresses during a cooling cycle (*1*). Different types of modifiers are usually added into AC mixes to improve their resistance to cracking. Accordingly, the addition of fibers

into AC mixtures has the potential to minimize the thermal and fatigue cracking distresses of asphalt pavement.

Several research studies have used fibers to enhance the cracking potential of asphalt mixes (2–5). According

¹Center for Research and Education in Advanced Transportation, Engineering Systems (CREATES), Rowan University, Glassboro, NJ

²Department of Civil and Environmental Engineering, Rowan University, Glassboro, NJ

³US Army Corps of Engineers, Engineering Research and Development Center, Cold Regions Research and Engineering Laboratory (CRREL), Hanover, NH

Corresponding Author:

Ayman Ali, alia@rowan.edu

to these studies, fibers reinforce the asphalt mixes three dimensionally and enhance the rutting and cracking resistance. Zarei et al. (6) studied the fracture behavior of fiber reinforcement into AC at intermediate and low temperatures using a semi-circular bend (SCB) test. The fracture behavior of warm mix asphalt (WMA) with the addition of polyester (PE) fibers was studied at -18°C and 25°C . Fibers of 8 mm length were added into the asphalt mix at 0.25% dosage by mix weight. According to numerical experimental results, SCB sample geometries in pure mode I (angular crack) and pure mode II (vertical crack) were able to characterize WMA fracture behavior at -18°C and 25°C . In addition, Zarei et al. reported that the distribution of coarse aggregate in the ligament area contributed toward fracture performance enhancement of WMA added mixtures. Overall, the addition of PE fibers showed the best results with respect to fracture mechanics. The low-temperature cracking resistance of Sasobit-coated aramid (SCA) fibers was assessed using the disk shape compact tension (DCT) test at -18°C and -24°C (7). Aramid fiber-reinforced mixtures were prepared using 19 mm long fibers and continuously fed into the mixing drum of the plant with the fiber delivery system. Reinforced mixtures on average showed 19% and 15% higher fracture energy at -24°C and -18°C , respectively, than that of the control mix. At -24°C and -18°C , the maximum crack mouth opening displacement (CMOD) increased by 11% and 13%, respectively. Both of these indicators showed that SCA fiber-reinforced asphalt mixtures (FRAMs) had better cracking resistance than the control mix.

Li et al. (8) examined the impact of basalt fiber reinforcement on low-temperature cracking performance. Basalt fibers of 9 mm length were added into the asphalt mix at 0%, 0.2%, 0.3%, 0.4%, and 0.5% dosage by mix weight. The thermal cracking performance was determined by performing the three-point bending beam (3PB) test at -10°C , -20°C , and -30°C . Bending stress and strain were computed by applying the constant loading rate of 50 mm/min. According to their research findings, Li et al. reported that bending stress had an increasing trend when the basalt fiber dosage increased from 0% to 0.5%, peaking at 0.4% dosage. The bending stress at 0.4% dosage increased by 16%, 12%, and 10% more than that of the control at -10°C , -20°C , and -30°C , respectively. The bending strain also had the same trend as that of the bending stress, that is, peaking at 0.4% dosage. On average, bending strain increased by 19%, 25%, and 29% corresponding to -10°C , -20°C , and -30°C , respectively, at 0.4% dosage. As the fiber dosage increases, fibers reinforce the mix three dimensionally and, once the dosage goes beyond an optimum level, the fibers start to pile up/clump, and thus the bending stress and bending strain reduce. Basalt fibers

improved the low-temperature cracking properties of FRAMs and change the failure mode from brittle to flexible (8).

In addition to fiber dosage and length, the distribution of fibers in asphalt mixtures is also a critical parameter that influences their fatigue and thermal cracking performance. Noorvand et al. (9) conducted a study to evaluate the impact of fiber state (distribution) for two different plant-produced FRAMs (Mix 1 and Mix 2) on the laboratory performance. The fiber distribution results showed that Mix 1 and Mix 2 had 89% and 16% fibers in the individual (distributed) state, respectively. At higher temperatures, Mix 1 yielded higher modulus values compared with Mix 2. In addition, Mix 1 showed 139% higher cycles in flow number (FN) compared with the control and Mix 2. Performance enhancement results showed that if the fibers were in a distributed state within an asphalt mixture, the rutting performance enhancement would be proportionate. Aramid fibers were treated with different types of coatings by Phan et al. (10) to study the effect of coating on fiber distribution. Uncoated aramid fibers as well as paraffin wax and warm mix asphalt (WMA) additives were added to the AC. Dry and wet mixing methods were utilized to mix fibers into the asphalt mixtures. Amongst both mixing methods, the wet mixing method showed consistent air voids for mix design samples. Therefore, laboratory performance samples were prepared using the wet mixing method. Phan et al. reported that wax, WMA, and uncoated aramid fibers showed 44%, 81%, and 48% higher cracking resistance, respectively, compared with the control mix. These FRAMs showed 18%, 45%, and 12% higher FN values, respectively, compared with the control mix. Phan et al. concluded that coating the aramid fibers with WMA additive minimized the connection between fibers and helped to produce FRAMs with homogenous fiber distribution.

Experimental variation (or testing variability) is also an important parameter to assess the consistency between different mechanical tests performed at low temperatures. The feasibility and variability of low-temperature fracture performance was evaluated using the indirect tensile strength (IDT) test, DCT test, and thermal stress restrained specimen test (TSRST) (11). The loading rate selected by the study (11) for the DCT and IDT tests were 0.017 mm/s and 12.5 mm/min, respectively. The IDT test was performed at 0°C , -10°C , and -20°C and, according to the results, different type of mixtures exhibits variable trend at 0°C and -10°C . TSRST critical cracking temperature results and DCT fracture energy results obtained at -18°C and -30°C were compared to determine the consistency of both performance tests. The TSRST critical cracking temperature and fracture energy results at -18°C showed a consistent trend; however,

Table 1. Properties of Fibers Used for the 9.5ME New Jersey Mix

Fiber property	Polyolefin/aramid	Sasobit-coated aramid
Specific gravity	0.91/1.44	1.44–1.45
Tensile strength (MPa)	483/3000	>2758
Length (mm)	19	19
Thickness (μm)	12	NA
Acid/alkali resistance	Inactive	NA
Decomposition temperature ($^{\circ}\text{C}$)	157/ >450	NA
Melting temperature ($^{\circ}\text{C}$)	150/350	77/350
Price (US\$/lb)	6.75	NA
Maximum recommended dosage rate ^a	0.05%	0.01% & 0.02%

Note: NA = not available.

^aRecommended dosage rate was obtained from the manufacturer and is presented as a percentage of total mix weight.

fracture energy determined at -30°C showed different ranking compared with the TSRST critical cracking temperature. Based on the fracture energy results comparison for the DCT and IDT tests with the TSRST critical cracking temperature, the results may be inaccurate to evaluate the low-temperature cracking performance of AC because the fracture energy in all of these experiments was mainly the surface energy (*II*). These findings are based on the fracture energy; however, the main performance indicators (i.e., indirect tensile strength (ITS), CT_{index} , and *FI*) were not considered for consistency comparison.

In general, the studies presented above showed the benefits of fiber length, dosage, and fiber distribution on low- and intermediate-temperature cracking performance for a given fiber type and experiment. In addition, the literature mentioned that different types of experiments may produce inconsistent results for the same mix type. However, few studies focused on exploring the low- and intermediate-temperature cracking behavior of reinforced mixes for a specific fiber type by using one test. Moreover, limited studies on plant-produced FRAMs are available in literature. Plant-produced mixes represent the actual mixing conditions of FRAMs (when compared to laboratory settings), which may ultimately lead to better fiber distribution. Therefore, this study explored the fatigue and thermal cracking behavior of aramid fibers combined with polyolefin (as a separator) and Sasobit (coating for better distribution) at different dosages. Finally, the findings of this study will be beneficial to the body of knowledge for managing roadways in different climatic regions.

Study Objectives

The goal of this study is to evaluate the intermediate (fatigue) and low-temperature (thermal) cracking performance of plant-produced FRAMs using different type of mechanical tests. The specific objectives include the following:

- determine the intermediate-temperature fatigue cracking performance of aramid fiber-reinforced asphalt mixes prepared at different dosages (0.01%, 0.02%, and 0.05%);
- evaluate the thermal cracking (low-temperature) performance of the control and FRAMs;
- compare the fatigue and thermal cracking performance of the control and FRAMs based on different mechanical tests; and,
- rank the different FRAMs based on their performance and identify the best fiber type and dosage.

Description of Material

One polymer modified binder (PG 76-22) commonly used in New Jersey (NJ), one aggregate type (diabase stone), and two different fibers (SCA fibers and polyolefin/aramid [PFA] fibers) were used to prepare a total of four asphalt mixtures (three FRAMs and one control without reinforcement). The physical properties of these fibers are shown in Table 1. All of these mixtures were prepared according to the NJ Department of Transportation (NJDOT) specification for a 9.5ME76 (i.e., air voids: $4 \pm 1\%$, min. Void in Mineral Aggregate (VMA): 15%, and N_{des} : 75 gyrations) mix. The gradation and optimum binder content used to prepare these mixtures are shown in Figure 1.

Four different mixes were prepared at a local asphalt batch plant in NJ. These mixtures included a control (no fiber) 9.5ME mix and three FRAMs (fibers and dosage: PFA at 0.05%, SCA at 0.01%, and SCA at 0.02%). All these mixtures were produced according to the manufacturer recommended fiber dosages. Different dry and wet mixing times were used at the batch plant. However, fibers were added into the mixing drum of the plant when heated aggregates were mixed (dry mixing). Once the dry mixing time was completed, the asphalt binder was added and mixing was carried out until the aggregates and fibers were coated well with the binder (wet mixing). All these mixtures were produced at mixing

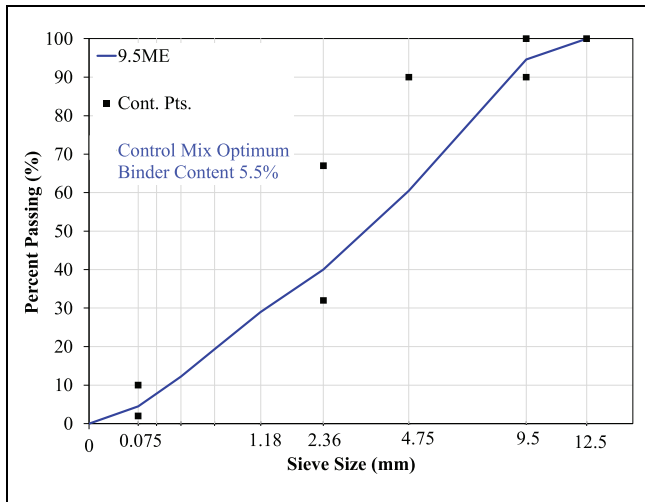


Figure 1. Gradation curve for 9.5ME New Jersey asphalt mix.

temperature of 160°C (320°F). The specific mixing times for each mix type are as follows:

- control and FRAM with PFA at 0.05% dosage: 5 s of dry mixing followed by 30 s of wet mixing;
- SCA mix at 0.01% dosage: 30 s of dry mixing followed by 30 s of wet mixing; and
- SCA mix at 0.02% dosage: 40 s of dry mixing followed by 30 s of wet mixing.

It is important to note that SCA fibers require additional dry mixing time compared with the control and PFA fibers. This is because the Sasobit coating of aramid fibers requires heat to melt the wax and distribute the fibers into the asphalt mix equally. Doubling the SCA dosage also required an additional 10-s dry mixing time. PFA fibers that contain polyolefin act as separator to keep aramid filaments separate and distributed equally into the mix. The main purpose of using a batch plant was to produce smaller quantities for comparing different mixtures (control and FRAMs) having the same gradation in laboratory testing settings. In the case of the drum plant, specialized fiber feeders are needed for continuous and accurate dosing of fibers into the asphalt mix, which may make the fiber distribution even better compared with the batch plant. The plant-produced mixtures were put into buckets, shipped to the laboratory, and their performance was evaluated at laboratory scale. Finally, for quality assurance of all mixture types, the binder content was determined by performing the ignition oven test (AASHTO T308). The binder contents in the control, PFA 0.05%, SCA 0.01%, and SCA 0.02% mixes were found to be 5.5%, 5.2, 5.5%, and 5.1%, respectively.

Laboratory Testing Program

The testing program adopted for this study is presented in Figure 2. After performing the superpave mix design, all mixtures (control and FRAMs) were prepared, and the ignition oven test was performed to ascertain the binder content of the mixes to assess their consistency (Figure 2). The plant-produced asphalt mixtures were heated in a forced draft oven at the compaction temperature 154°C (310°F) and once the mix reached the compaction temperature the samples were compacted in a Superpave Gyratory Compactor (SGC) to determine the laboratory performance. As shown in Figure 2, the DCT test and TSRST were performed to evaluate the low-temperature thermal cracking performance of the FRAMs. The intermediate-temperature cracking performance was determined by performing the indirect tension asphalt cracking test (IDEAL-CT), SCB test, 3PB test and uniaxial fatigue test (Figure 2). The comparison of low and intermediate performance testing will provide the impact of fiber reinforcement at different dosages by mix weight. In addition to dosage, this comparison will determine the impact of adding different combinations (polyolefin and Sasobit) of aramid fibers. The detailed testing procedure is explained in the following section.

Indirect Tension Asphalt Cracking Test (ASTM D8225)

The IDEAL-CT was performed to evaluate the cracking performance of asphalt mixtures at an intermediate test temperature (25°C) (12). Three samples were fabricated in the SGC at a target air void level of $7 \pm 0.5\%$, with a diameter of 150 mm and a height of 62 mm. A constant loading rate of 50 mm/min was applied diametrically on the samples until failure. Load and displacement data were recorded throughout the test and plotted to get the load–displacement curve. Several cracking performance parameters were calculated, including fracture energy G_f (area under the load displacement curve), crack propagation rate ($|m_{75}|$), ductility of the mix (l_{75}), ITS and the crack tolerance index (CT_{index}). Higher G_f , l_{75} , ITS, and CT_{index} and lower $|m_{75}|$ indicate better resistance of the mix to cracking.

Semi-Circular Bend Test (AASHTO T 393)

The SCB test evaluates the cracking performance of the asphalt mix at intermediate temperatures (25°C) using notched samples. According to AASHTO T 393 (13), samples were compacted with a diameter of 150 mm and to a height of 160 mm. The samples were sliced into 50 mm thickness, halved, and notched to a 15 mm length. All the specimens were subjected to meet a target air void level of $7 \pm 0.5\%$. Three samples were subjected to a

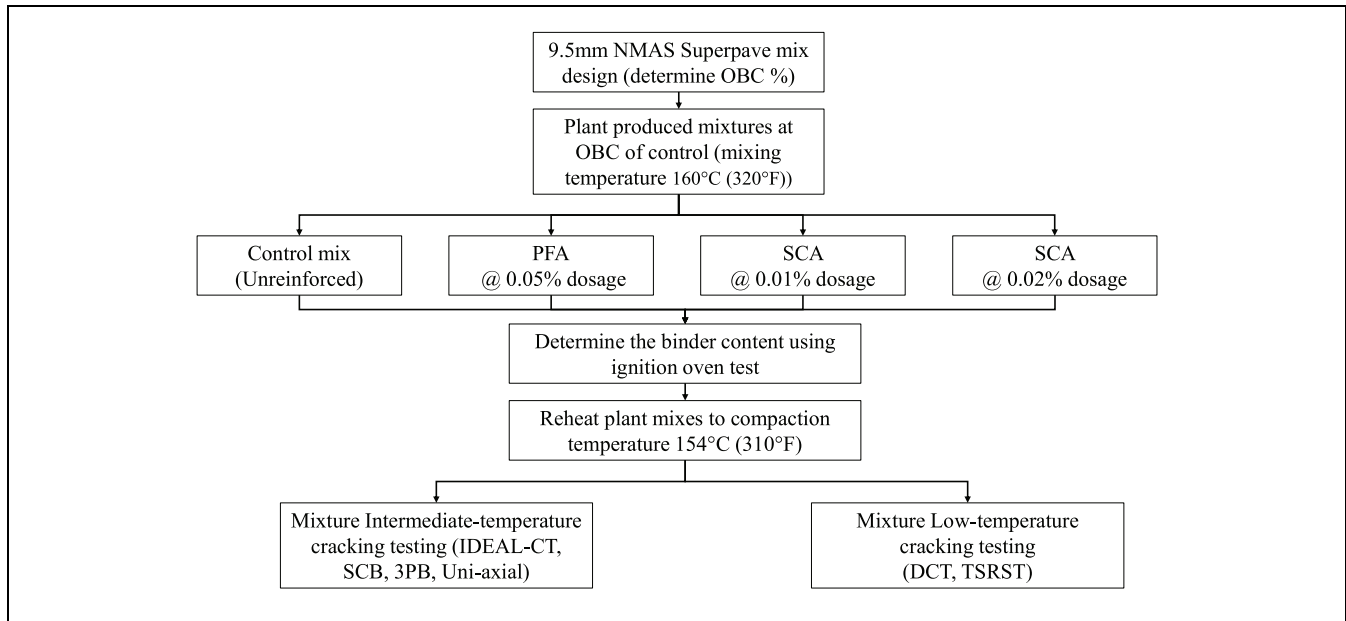


Figure 2. Testing program adopted to evaluate the cracking performance.

Note: NMAS = Nominal maximum aggregate size; OBC = Optimum binder content; PFA = polyolefin/aramid; SCA = Sasobit-coated aramid; IDEAL-CT = indirect tension asphalt cracking test; SCB = semi-circular bend; 3PB = three-point bending beam; DCT = disk shape compact tension; TSRST = thermal stress restrained specimen test.

constant loading rate of 50 mm/min until failure and load–displacement curves were plotted from the collected data. The fracture energy G_f and slope of inflection point ($|m|$) on the post-peak curve were computed from the load–displacement curve. The ratio of both these parameters provides the FI , an index to quantify the cracking resistance. Higher values of G_f and FI and lower value of $|m|$ represent better cracking resistance of the mix.

Three-Point Bending Beam Test

The purpose of this test was to determine the cracking resistance of the asphalt mixture under flexural loading. The 3PB loading jig was fabricated as per the literature (14, 15) and is shown in Figure 3. The fixture was mounted to the base of a servo-hydraulic loading frame, and samples were loaded at a constant displacement rate of 5 mm/min. This loading rate was selected from the literature (15). Beams were compacted in a vibratory compactor and cut into final dimensions of 380 ± 6 mm by 63 ± 2 mm by 50 ± 2 mm in accordance with the AASHTO T321 specification. A target air void level of $7 \pm 0.5\%$ was used for preparing these samples. To ensure that a crack initiates from the selected desired location, a 5 mm notch was created at the bottom middle of the beam. Samples were conditioned at $25 \pm 1^\circ\text{C}$ for 2 h. Three replicates of each mix types were tested, and the test was terminated once the load dropped to 0.1 kN. The load–displacement curve was obtained from the collected data and different cracking parameters were

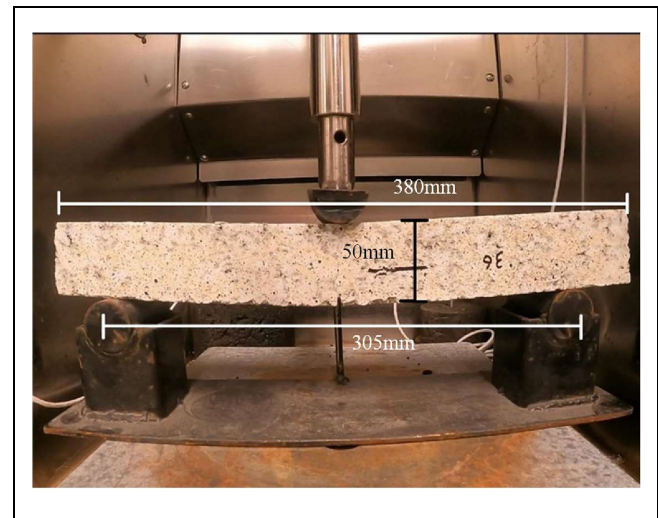


Figure 3. Image of the three-point bending beam experimental setup with the jig.

computed from this curve, including the fracture energy G_f and peak load. Higher values of G_f and peak load indicate better cracking performance of the asphalt mix.

Uniaxial Fatigue Test (AASHTO TP 107)

The uniaxial fatigue test was performed according to AASHTO TP 107 (16). Three test specimens of 130 mm height and 100 mm diameter were fabricated in the lab with the target air void level of $7 \pm 0.5\%$. Epoxy was

applied on both the ends and loading platens were connected to apply the tensile load at 10 Hz frequency. The peak-to-peak microstrains were set to $400\ \mu\epsilon$. Finally, the damage characteristic (pseudo stiffness $[C]$ versus damage parameter $[S]$) curve was plotted to characterize the performance of different mixtures. A longer C versus S curve indicates better fatigue behavior of the asphalt mixtures.

Disk Shaped Compact Tension Test (ASTM D7313-13)

The DCT test was performed to evaluate the fracture resistance of unreinforced (control) and reinforced asphalt mixtures at low temperature. According to ASTM D7313-12 (17), three replicates of 50 mm height were fabricated in the laboratory at a target air void level of $7 \pm 0.5\%$. The samples were tested at -12°C for PG 76-22, which is a 10°C warmer temperature than the low performance grading (PG) value of the binder. The test was conducted with a constant CMOD rate of 1 mm/min. The test was terminated when the load reduced to 0.1 kN, and the load–CMOD curve was obtained from the recorded data. The fracture energy (G_f), peak load, and maximum CMOD (the point where the load reach to 0.1 kN) values were calculated from the load–CMOD curve to determine the thermal cracking behavior of the FRAMs. Higher values of G_f , peak load, and maximum CMOD represent higher resistance of the mix to thermal cracking.

Thermal Stress Restrained Specimen Test (AASHTO TP-10)

The purpose of this test was to determine the thermal cracking performance of asphalt mixtures when cooled at a constant rate. Three replicates with 250 mm by 50 mm by 50 mm dimensions were fabricated and tested according to AASHTO TP-10 (18). The samples were glued with aluminum plates and cooled from 10°C to -50°C at a rate of $10^\circ\text{C}/\text{h}$. As the temperature drops, asphalt samples contract while being restrained from both edges. Tensile stress is induced in the asphalt specimen when it undergoes thermal contraction. Once the tensile stress exceeds the material's strength, the sample breaks. This test measures the critical cracking temperature (T_c), tensile strength, and fracture energy (G_f) at failure. A lower failure temperature, higher tensile strength, and higher fracture energy indicate better resistance of the asphalt to thermal cracking.

Results and Discussion

Impact of Fiber Reinforcement on Cracking Performance

The intermediate cracking test (3PB, IDEAL-CT, and SCB) results for all types of plant mixtures are shown in Figure 4. Figure 4a presents the 3PB test results. As

illustrated in this figure, the fracture energy for the FRAMs is higher than that of the control mix. This suggests that the unreinforced (control) mix has lower cracking resistance compared with the FRAMs. This was the case because aramid fibers helped the mix resist crack initiation and propagation. In addition, the SCA 0.02% fibers exhibits the highest fracture energy because the probability of fibers being in the crack path increases compared with the other reinforced mixtures. However, for PFA 0.05% the proportion of aramid fibers is $<25\%$ of the total PFA weight and significantly lower than the SCA fibers. Furthermore, asphalt mixtures reinforced with PFA and SCA fibers reinforced at 0.05% and 0.02% dosages, respectively, showed higher peak load (see Figure 4a). This indicates that FRAMs perform better with respect to fatigue cracking performance at intermediate temperature.

Figures 4, b and c, presents the results of ITS and IDEAL-CT testing. According to Figure 4b, it is observed that all FRAMs are showing approximately similar ITS values compared with the control mix. While this observation indicates that all mixes might have a similar ability to resist cracking, it is noted that ITS alone may not be a good indicator for assessing the cracking resistance of asphalt mixtures (19). In addition to ITS, Figure 4c presents the results of the CT_{index} obtained from the IDEAL-CT. As illustrated in this figure, SCA fiber-reinforced mixes at 0.01% and 0.02% dosages show approximately 1.2 times and 1.4 times higher CT_{index} values, respectively, compared with the control mix. This implies that the cracking performance of these two FRAMs increases proportionally with doubling the dosage. In case of the PFA-reinforced mix, although the dosage is 0.05%, the lower binder content (5.2% compared to control of 5.5%) for plant mixtures might be the reason for having equivalent cracking performance for the PFA-reinforced mix, thus explaining why the performance of the PFA FRAM is similar to that of the control mix with respect to the IDEAL-CT results.

The SCB test results for the flexibility index (FI) are depicted in Figure 4d. As illustrated in this figure, the SCA-reinforced mix at 0.02% dosage showed higher (1.5 times) FI values compared with the control mix. Similar to the IDEAL-CT results (Figure 4c), this observation indicates better cracking resistance for the SCA 0.02% reinforced mix. The lower binder content for the PFA-reinforced mix caused the reduced cracking resistance. This observation indicates that the SCB test can better identify the variability of different mixes. Except for the SCA 0.01% FRAM, all other mixtures are showing the same ranking for the CT_{index} and FI . The SCA 0.01% FRAM shows a different ranking because the SCB test was performed on notched samples and did not account

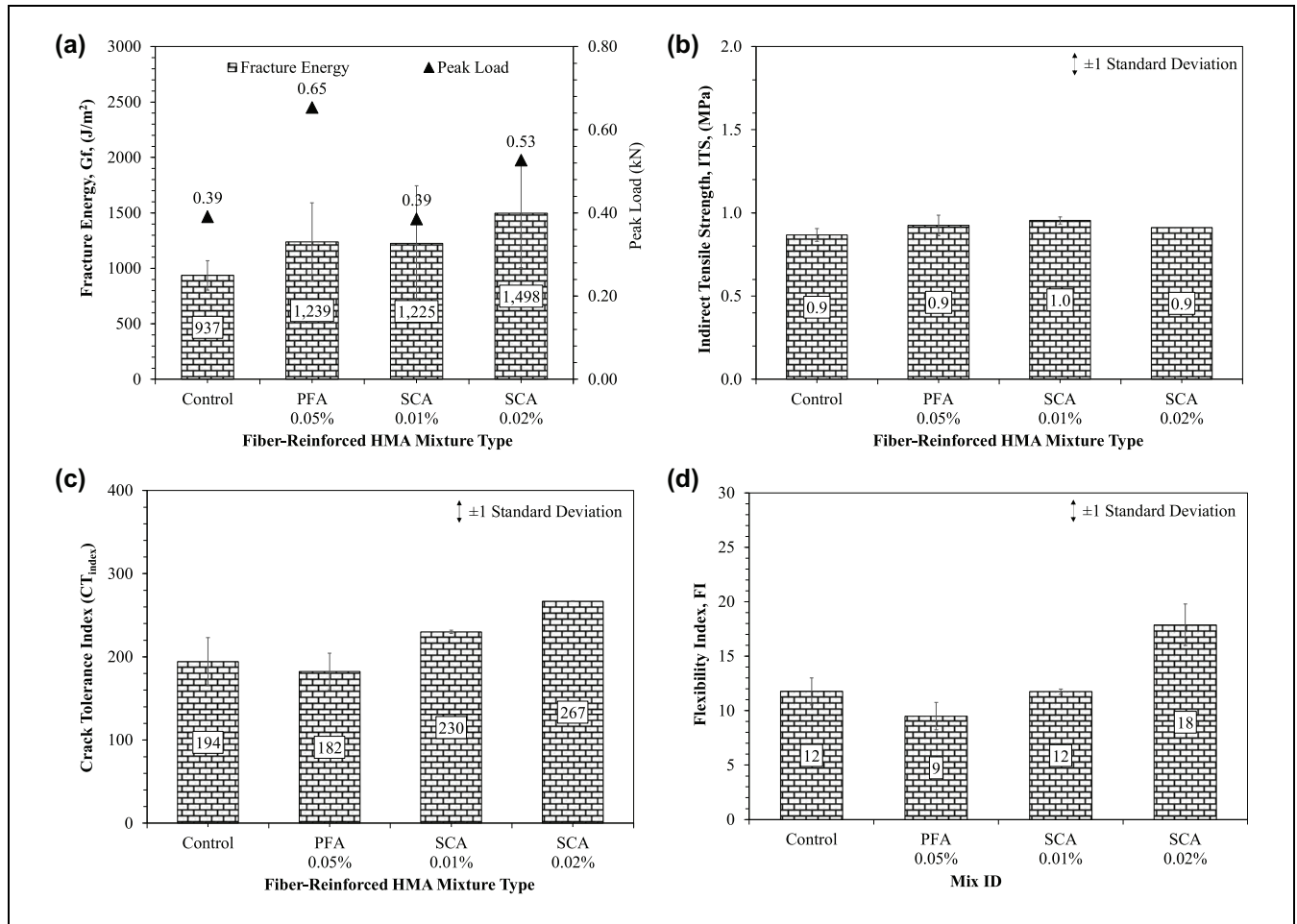


Figure 4. Intermediate-temperature cracking test results: (a) three-point bending beam test results; (b) indirect tension asphalt cracking test (IDEAL-CT) indirect tensile strength (ITS) results; (c) IDEAL-CT CT_{index} ; (d) semi-circular bend test FI results.

Note: PFA = polyolefin/aramid; SCA = Sasobit-coated aramid; HMA = hot mix asphalt.

for the crack initiation in the fracture process; however, the IDEAL-CT includes both crack initiation and crack propagation phases.

To characterize the behavior of fiber reinforcement on each parameter of the CT_{index} and FI of the asphalt mixtures, the results were further analyzed using interaction charts. Figure 5a represents the interaction chart for the CT_{index} built by plotting G_f on the y-axis and $l_{75}/|m_{75}|$ on the x-axis. The higher G_f and $l_{75}/|m_{75}|$ values yielded a higher CT_{index} and are located on the upper right corner of the interaction diagram. On the other hand, an interaction chart for the SCB test was also developed to identify the impact of fiber reinforcement and assess the consistency between the experiments. The G_f values were plotted on the y-axis and the $|m|$ values were plotted on the x-axis. Whereas G_f indicates the toughness of the mixtures, $l_{75}/|m_{75}|$ and $|m|$ represent the ductile-brittle behavior. Higher values of $l_{75}/|m_{75}|$ and lower values of $|m|$ imply that the asphalt mixture exhibits ductile behavior, and vice versa.

Figures 5, a and b, indicates the results of the IDEAL-CT and SCB test of unreinforced and reinforced asphalt mixtures on the performance interaction chart, respectively. As shown, PFA-reinforced asphalt mixtures showed higher G_f values for both the IDEAL-CT and SCB test compared with the control mix. In addition, PFA-reinforced mixtures showed lower ($l_{75}/|m_{75}|$) values (see Figure 5a) and higher $|m|$ values (Figure 5b). These observations demonstrate that PFA reinforcement increased the toughness of the mix and showed brittle behavior compared with the control mix. In addition to the PFA-reinforced mix, SCA fibers at both dosages (0.01% and 0.02%) showed higher G_f values for the IDEAL-CT (Figure 5a) and SCB test (Figure 5b). The addition of SCA fibers increased the toughness of the mix. However, SCA fibers at a higher dosage (0.02%) showed significantly high $l_{75}/|m_{75}|$ (Figure 5a) and low $|m|$ value (Figure 5b). Both of these observations suggest that the addition of aramid fibers coated with Sasobit at higher dosage improved the ductility of the mix.

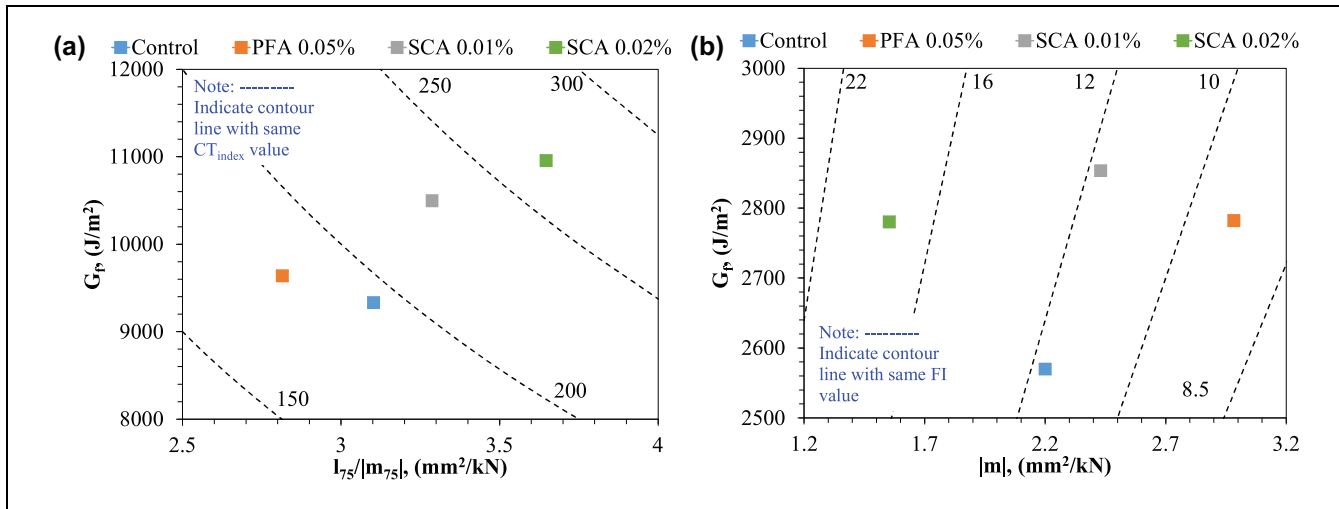


Figure 5. Performance interaction charts: (a) indirect tension asphalt cracking test results interaction chart; (b) semi-circular bend test results interaction chart.

Note: PFA = polyolefin/aramid; SCA = Sasobit-coated aramid.

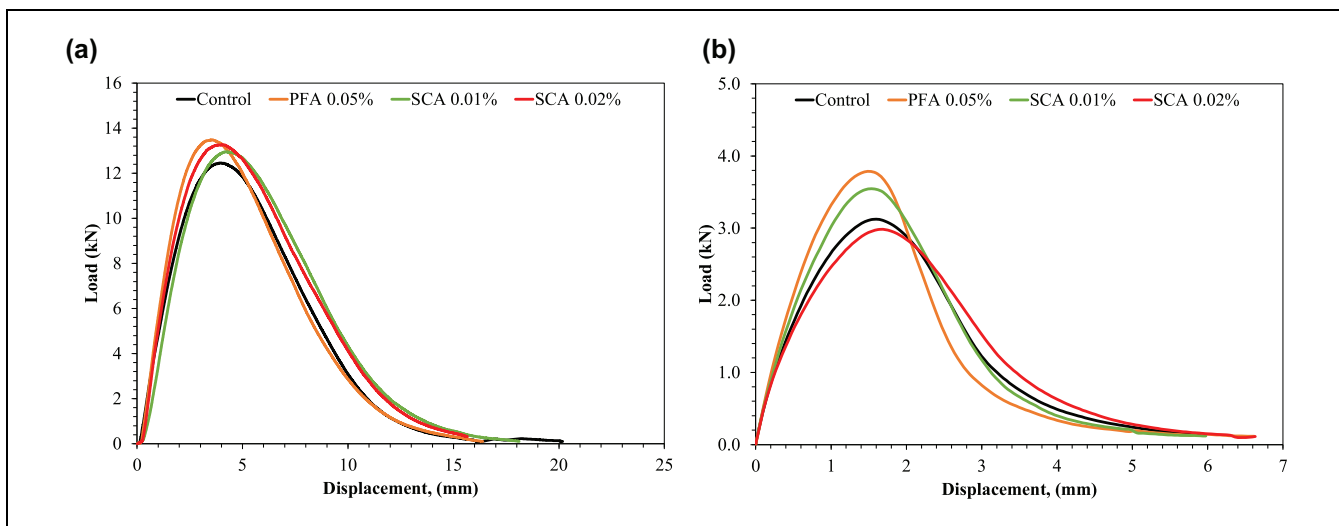


Figure 6. Load versus displacement curves: (a) indirect tension asphalt cracking test; (b) semi-circular bend test.

Note: PFA = polyolefin/aramid; SCA = Sasobit-coated aramid.

However, the SCA 0.01% reinforced mix showed similar ductile behavior compared with the control mix (Figures 5, *a* and *b*). The performance interaction chart results indicates that both the IDEAL-CT and SCB test showed consistent behavior of the unreinforced and reinforced mixes. Figures 6, *a* and *b*, represents the load–displacement curves for the IDEAL-CT and SCB test, respectively. Both of these figures indicate that the PFA 0.05% and SCA 0.01% reinforced mixtures are showing a higher peak load compared with the control mix. The SCA-reinforced mixtures after peak load (once crack generated) show delayed crack propagation compared with the control and PFA mix. However, the peak loads

and displacements for the IDEAL-CT (see Figure 6*a*) are three to four times higher than those of the SCB test (see Figure 6*b*). This is because the SCB samples are notched and do not require load to initiate a crack, but in the case of the IDEAL-CT, crack initiation occurs as the samples are not notched.

Figure 7 shows the results of the uniaxial fatigue test. The pseudo stiffness versus damage characteristic curve is shown for the control and FRAMs. According to this figure, all types of reinforced mixtures showed higher stiffness and damage compared with the control mix. This shows that a fiber-reinforced mix under tensile loading resists deformation, which causes the mix to have

higher stiffness. However, the control mix did not have any reinforcement, which causes the mix to have a lower damage characteristic curve (Figure 7). Overall, SCA fibers at the 0.01% dosage showed the highest improvement, because the binder content is equivalent to the control mix; however, in case of the PFA 0.05% and SCA 0.02% reinforced mixtures, the binder content is lower than that of the control mix.

Impact of Fiber Reinforcement on Low-Temperature (Thermal) Cracking

Figure 8 presents the results (DCT test and TSRST) of thermal cracking for the control and FRAMs. Figure 8a shows the fracture energy (G_f) results obtained from the

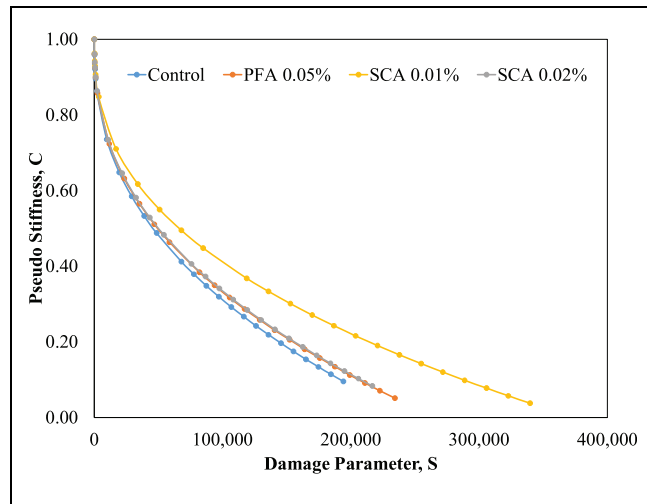


Figure 7. Uniaxial fatigue test results.

Note: PFA = polyolefin/aramid; SCA = Sasobit-coated aramid.

DCT test conducted at -12°C . All of the reinforced mixtures are showing higher (approximately 1.2–1.4 times) fracture energies compared with the control mix. This illustrates better thermal cracking behavior for the FRAMs. This improvement is attributed to the fiber reinforcement, which resists crack initiation and propagation even at low temperatures. However, SCA fiber-reinforced mixes showed the highest improvement in low-temperature cracking resistance, regardless of dosage. Besides fracture energy (G_f), Figure 8b represents the results for peak load required to initiate the crack. In this figure, only the PFA 0.05% and SCA 0.02% FRAMs show a higher peak load compared with the control mix. This was because a higher dosage of fibers resists crack initiation and a higher load is required to generate the crack.

The low-temperature cracking behavior of the FRAMs was also assessed by performing the TSRST and Figure 9 shows the TSRST results (G_f , ultimate load, and critical cracking temperature). It can be seen from Figure 9a that the FRAMs showed on average slightly higher (by almost 1.07 times) fracture energy. This observation indicates that, with respect to fracture energy, the TSRST was unable to capture the behavior of the FRAMs. In comparison to fracture energy, the FRAMs are showing higher peak load (approximately 1.3–1.4 times) compared with the control mix (see Figure 9b). The higher peak loads are demonstrating better thermal cracking performance of the FRAMs. Similar findings are observed for critical temperature ($T_c^{\circ}\text{C}$) at sample failure, as shown in Figure 9c. It can be seen from this figure that the FRAMs fail between -28°C and -30°C compared with the control mix, which fails at -23°C . This suggests that the FRAMs deter crack formation by resisting crack formation at lower temperatures.

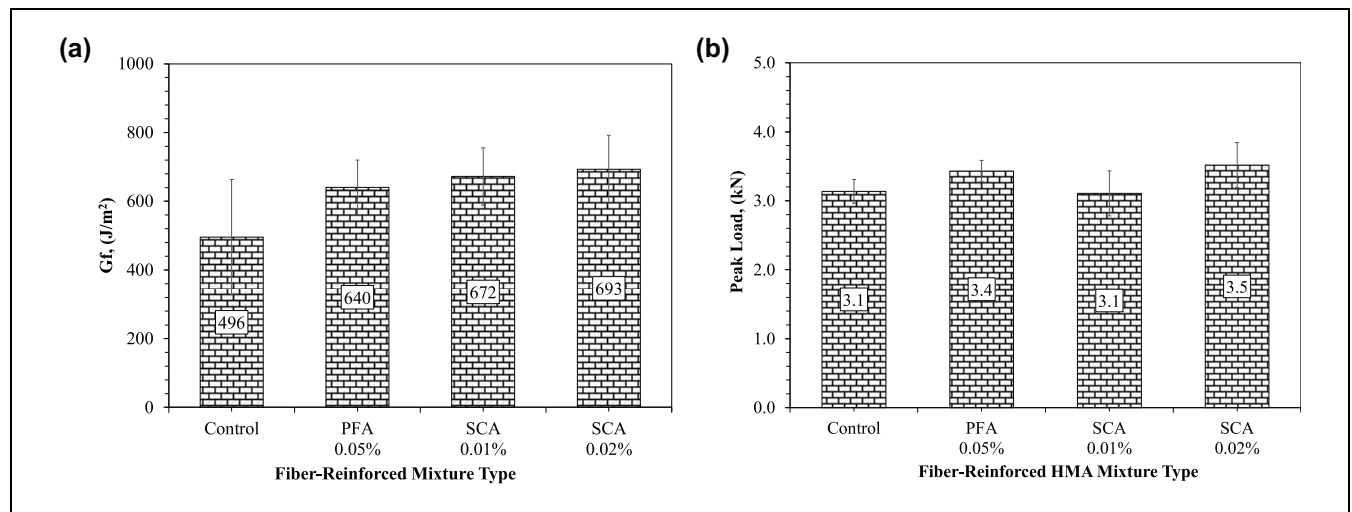


Figure 8. Disk shape compact tension test results: (a) fracture energy; (b) peak load.

Note: PFA = polyolefin/aramid; SCA = Sasobit-coated aramid; HMA = hot mix asphalt.

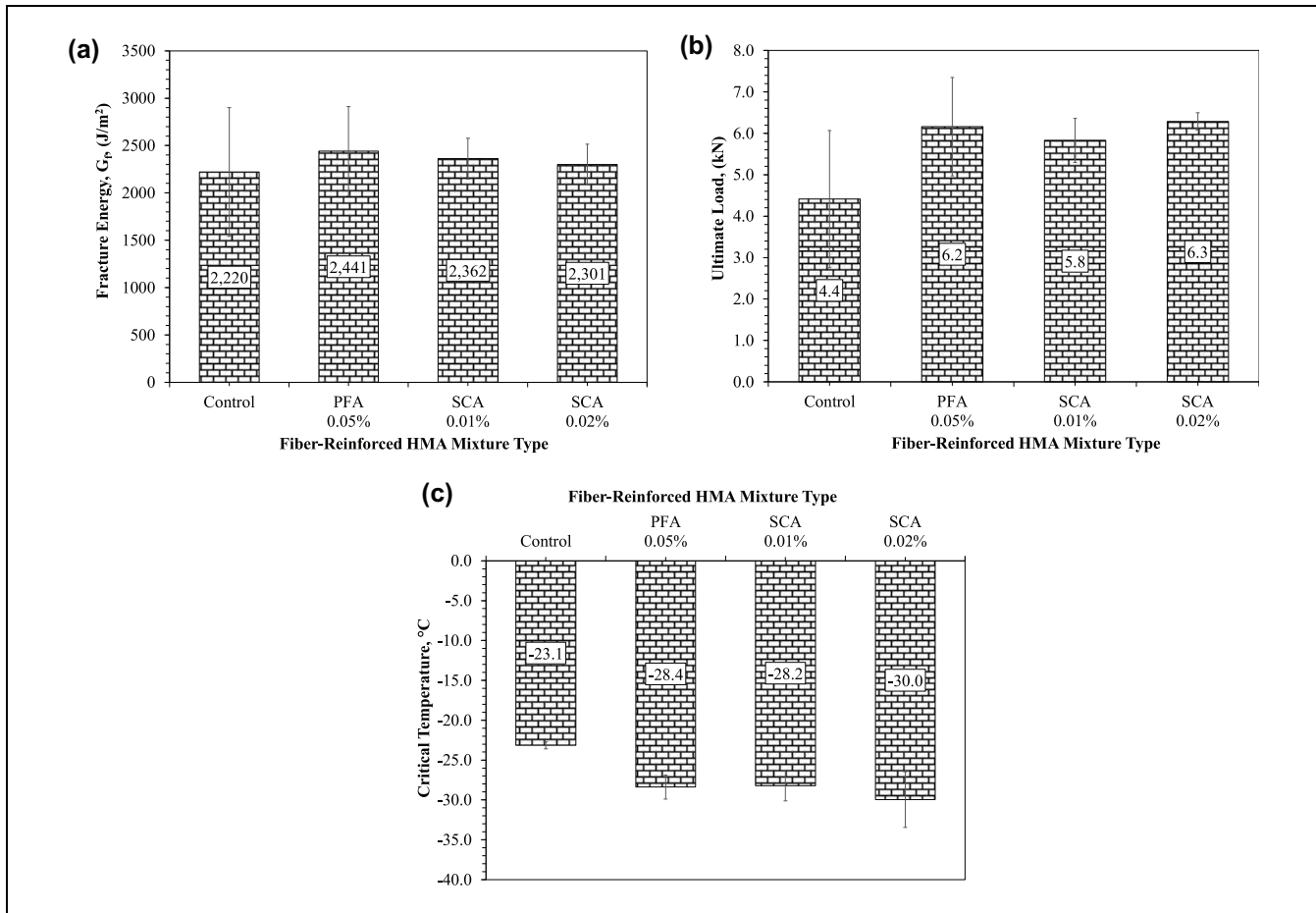


Figure 9. Thermal stress restrained specimen test results: (a) fracture energy; (b) ultimate load; (c) critical cracking temperature.

Note: PFA = polyolefin/aramid; SCA = Sasobit-coated aramid; HMA = hot mix asphalt.

Ranking Based on Mixture Test Results and Statistical Analysis

Typically, radar charts were developed for rigorous financial analysis and to allow for comparing different parameters simultaneously (1, 20). As this study includes different parameters for evaluating the low- and intermediate-temperature cracking properties of the asphalt mixtures, these charts were found to be useful to compare different indicators of the control and FRAMs. Five parameters, namely the FI , CT_{index} , TSRST T_c ($^{\circ}C$), TSRST fracture energy, and DCT fracture energy, were used to identify the optimum performing mixture. For simplicity, all performance indicators were normalized between 0 and 1.0. In addition, equal areas bounded by each polygon were calculated to rank the different FRAMs. Figures 10, *a–d*, indicates the separate radar charts for the control and FRAMs plotted on the same scale. As can be seen in Figure 10*c*, the SCA 0.01% FRAM showed highest fracture energy for the DCT test at $-12^{\circ}C$ followed by the SCA 0.02% FRAM. In the case

of the TSRST, which includes temperatures from $+10^{\circ}C$ to $-50^{\circ}C$, the PFA 0.05% FRAM showed the higher TSRST fracture energy compared with the other mix types (See Figure 10*b*). Finally, the SCA 0.02% FRAM indicated the best improved behavior in three parameters (FI , CT_{index} , and TSRST T_c [$^{\circ}C$]), as shown in Figure 10*d*. Figures 10, *c* and *d*, indicates that the SCA 0.02% mixtures bounded the highest region, followed by the SCA 0.01% mixtures, compared with the control. This observation suggests as the SCA fiber dosage increases, the overall performance increases proportionately.

Table 2 presents an analysis of variance (ANOVA) conducted for laboratory experiments. The FI and CT_{index} test results indicate that a statistically significant ($F = 17.9$, $\alpha = 0.001$ and $CT_{index} F = 13.2$, $\alpha = 0.002$) difference was found. These findings illustrate that fiber-reinforced mixtures show significantly different results. In addition, the TSRST critical cracking temperature (T_c) also shows statistically significant ($F = 5.7$, $\alpha = 0.022$) different results compared with the control

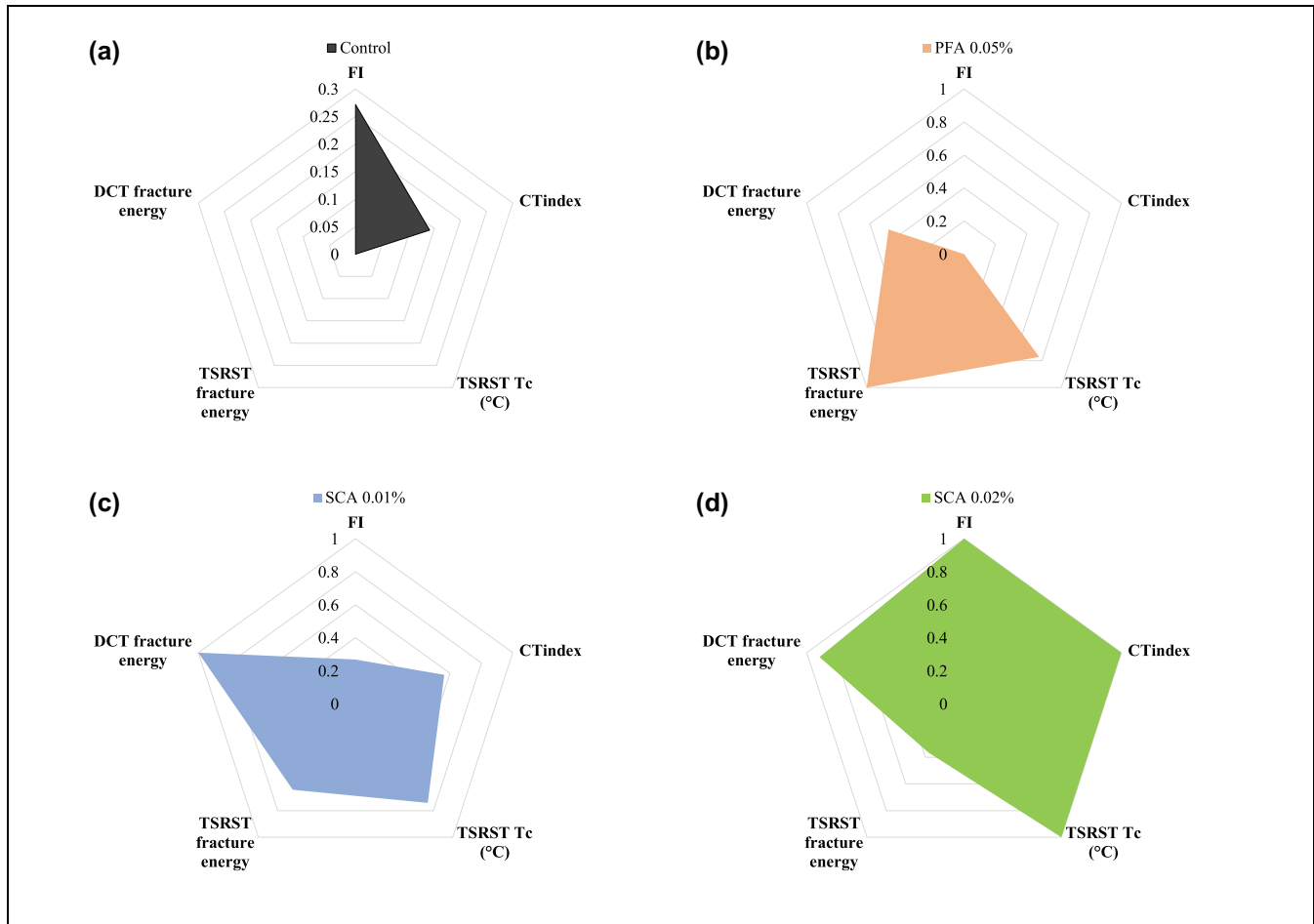


Figure 10. Performance diagram radar chart: (a) control; (b) polyolefin/aramid (PFA) 0.05%; (c) Sasobit-coated aramid (SCA) 0.01%; (d) SCA 0.02%.

Note: DCT = disk shape compact tension; TSRST = thermal stress restrained specimen test; FI = flexibility index.

Table 2. Analysis of Variance (ANOVA) for Laboratory Performance Test Results of Fiber-Reinforced Asphalt Mixtures

Statistical factor	<i>F</i>	Sig (α)
<i>FI</i>	17.9	0.001*
<i>CT_{index}</i>	13.2	0.002*
3PB <i>G_f</i>	2.5	0.125
TSRST <i>T_c</i>	5.7	0.022*
DCT <i>G_f</i>	0.5	0.684

Note: 3PB = three-point bending beam; DCT = disk shape compact tension; TSRST = thermal stress restrained specimen test; FI = flexibility index; CT = cracking test; Sig = significance.

*Statistically significant at 95% confidence level.

mix, whereas, in the case of the 3PB and DCT test results, both indicate statistically insignificant (3PB G_f $F = 2.5$, $\alpha = 0.125$ and DCT G_f $F = 0.5$, $\alpha = 0.684$) differences between unreinforced (control) and reinforced mixtures. This indicates that both the DCT and 3PB

tests did not show significantly different results compared with the control mix.

Summary, Conclusions, and Recommendations

This study evaluated the intermediate- (fatigue) and low-temperature (thermal) cracking performance of FRAMs. In addition, the impact of aramid fibers along with different combinations (polyolefin and Sasobit wax) on the fatigue and thermal cracking performance of FRAMs was studied. PFA was added to the asphalt mix at 0.05% dosage and SCA fibers were added at 0.01% and 0.02% dosages. All of these mixes are produced at a plant to represent the actual mixing conditions. Laboratory intermediate cracking resistance was determined using the IDEAL-CT, SCB test, and 3PB test; low-temperature cracking performance was evaluated using the DCT test

and TSRST. The following conclusions were drawn based on the laboratory experimental results.

- The addition of aramid fibers into asphalt mixtures improves the fatigue cracking of these mixtures at intermediate testing temperatures according to the 3PB test results. This was because the fibers are in the distributed state in the asphalt mix and resist the deformation of the mix.
- The IDEAL-CT and SCB test results showed that SCA fibers, regardless of dosage, improved the intermediate cracking resistance. The performance is proportionate as the dosage doubled. This was because the aramid fibers resist crack initiation and propagation. However, PFA fiber-reinforced mixtures at 0.05% dosage tend to have similar cracking performance. This was because the PFA-reinforced mixture had (0.3%) lower binder content than the control mix.
- The performance interaction charts provide a more comprehensive interpretation of the IDEAL-CT and SCB test results. The interaction charts showed higher (G_f) values for the FRAMs compared with the control mix. PFA 0.05% reinforced mixtures show brittle behavior (lower $l_{75}/|m_{75}|$ and higher $|m|$ value) but SCA fibers, regardless of dosage, improved the ductile behavior of the FRAMs. Therefore, SCA fibers showed improved intermediate-temperature cracking performance.
- Uniaxial fatigue test results showed improved fatigue performance of the FRAMs. Regardless of combination and dosage, the FRAMs showed an improvement with respect to a higher pseudo stiffness and damage parameter. This is because aramid fibers resist the deformation of the mix under tensile loading.
- The DCT test results indicated that with addition of fibers into the asphalt mix, the low-temperature cracking performance improved based on the G_f values, while SCA fibers at 0.01% dosage showed the best performance at -12°C . The main reason for this improvement is associated with fiber reinforcement, which resists crack initiation effectively under tensile loading and requires higher fracture energy to fracture the mix.
- Overall, based on the TSRST results, all type of FRAMs showed better thermal cracking performance compared with the control mix. Based on G_f , ultimate load at fracture and critical cracking temperature indicators of the SCA fibers at 0.02% dosage and PFA fibers at 0.05% dosage showed the best thermal cracking performance. At higher dosage, fibers helped the mix to resist tensile loading and delay the crack initiation.

- The main performance indicator for each test ranking analysis was assessed. The performance charts indicate that SCA fibers at 0.02% dosage by mix weight showed the best low- and intermediate-temperature cracking behavior followed by the SCA 0.01%, PFA 0.05%, and control (unreinforced). This also indicates that the addition of aramid fibers helped the mix to enhance the cracking properties (both fatigue and thermal) of asphalt mixtures, regardless of dosage.
- The performance chart results shows that the SCB FI , IDEAL-CT CT_{index} , and TSRST critical fracture temperature produces consistent ranking for different types of mixes. However, the DCT G_f and TSRST G_f showed inconsistent ranking for the FRAMs. However, all laboratory experiments are able to characterize the behavior of the FRAMs.

Overall, the findings of this study are limited to a specific asphalt mix, mixing method, and fiber reinforcement. The future research plan includes the exploration of different fiber types and treatment types to understand the role of fibers and treatments on fiber distribution. In addition, a laboratory experimental investigation considering different fiber lengths would help one to understand the impact of fiber length on asphalt mix properties.

Acknowledgments

Special thanks are due to Keith Sterling from AE Stone, Scott Nazar from Forta, and Steve Santa Cruz from Surface Tech for providing the materials used in this study.

Author Contributions

The authors confirm contribution to the paper as follows: study conception and design: A. Raza Khan, A. Ali; data collection: A. Raza Khan, A. Ali, M. Elshaer; analysis and interpretation of results: A. Raza Khan, A. Ali, M. Elshaer; draft manuscript preparation: A. Raza Khan, A. Ali, Y. Mehta. All authors reviewed the results and approved the final version of the manuscript.

Declaration of Conflicting Interests


The author(s) declared no potential conflicts of interest with respect to the research, authorship, and/or publication of this article.


Funding

The author(s) disclosed receipt of the following financial support for the research, authorship, and/or publication of this article: The work described in this paper was conducted at Rowan University's Center for Research and Education in Advanced Transportation Engineering Systems (CREATES),

Mullica Hill, NJ. The experiments described and the resulting data presented in the article, unless otherwise noted, were funded under PE 0602784A, Project T53 “Military Engineering Applied Research,” Task 08 under Contract W913E521C0020, managed by the U.S. Army Engineer Research and Development Center (ERDC). Permission was granted by the Director of Geotechnical and Structures Laboratory to publish this information.

ORCID iDs

Ayman Ali  <https://orcid.org/0000-0002-7031-4852>

Yusuf Mehta  <https://orcid.org/0000-0001-9430-3827>

Data Accessibility Statement

The data presented in this manuscript can be accessed on request from and approval of the corresponding author.

References

- Kabir, S. F., A. Ali, C. Purdy, C. Decarlo, M. Elshaer, and Y. Mehta. Thermal Cracking in Cold Regions’ Asphalt Mixtures Prepared Using High Polymer Modified Binders and Softening Agents. *International Journal of Pavement Engineering*, 2022, pp. 1–9. <https://doi.org/10.1080/10298436.2022.2147523>.
- Asghar, M. F., M. J. Khattak, and A. Olayinka. Evaluation of Fracture Performance of Polyvinyl Alcohol Fiber Reinforced Hot Mix Asphalt. *Construction and Building Materials*, Vol. 350, 2022, p. 128741.
- Asghar, M. F., and M. J. Khattak. Evaluation of Mixture Design and Tensile Characteristics of Polyvinyl Alcohol (PVA)–Fiber Reinforced HMA Mixtures. *International Journal of Pavement Research and Technology*, 2022, pp. 1–22. <https://doi.org/10.1007/s42947-022-00233-3>.
- Alfalalah, A., D. Offenbacher, A. Ali, C. Decarlo, W. Lein, Y. Mehta, and M. Elshaer. Assessment of the Impact of Fiber Types on the Performance of Fiber-Reinforced Hot Mix Asphalt. *Transportation Research Record: Journal of the Transportation Research Board*, 2020. 2674: 337–347.
- Alfalalah, A., D. Offenbacher, A. Ali, Y. Mehta, M. Elshaer, and C. Decarlo. Evaluating the Impact of Fiber Type and Dosage Rate on Laboratory Performance of Fiber-Reinforced Asphalt Mixtures. *Construction and Building Materials*, Vol. 310, 2021, p. 125217. <https://doi.org/10.1016/j.conbuildmat.2021.125217>.
- Zarei, M., A. Abdi Kordani, M. Zahedi, F. Akbarinia, and M. Khanjari. Evaluation of Low and Intermediate Temperatures Fracture Indices for Modified Warm Mix Asphalt (WMA) Using Edge Notched Disc Bend (ENDB) Specimen. *Theoretical and Applied Fracture Mechanics*, Vol. 116, 2021, p. 103137. <https://doi.org/10.1016/j.tafmec.2021.103137>.
- Ge, D., D. Jin, C. Liu, J. Gao, M. Yu, L. Malburg, and Z. You. Laboratory Performance and Field Case Study of Asphalt Mixture with Sasobit Treated Aramid Fiber as Modifier. *Transportation Research Record: Journal of the Transportation Research Board*, 2022. 2676: 811–824. <https://doi.org/10.1177/03611981211047833>.
- Li, Z., A. Shen, H. Wang, Y. Guo, and H. Wu. Effect of Basalt Fiber on the Low-Temperature Performance of an Asphalt Mixture in a Heavily Frozen Area. *Construction and Building Materials*, Vol. 253, 2020, p. 119080. <https://doi.org/10.1016/j.conbuildmat.2020.119080>.
- Noorvand, H., R. Salim, J. Medina, J. Stempihar, and B. S. Underwood. Effect of Synthetic Fiber State on Mechanical Performance of Fiber Reinforced Asphalt Concrete. *Transportation Research Record: Journal of the Transportation Research Board*, 2018. 2672: 42–51.
- Phan, T. M., S. N. Nguyen, C. B. Seo, and D. W. Park. Effect of Treated Fibers on Performance of Asphalt Mixture. *Construction and Building Materials*, Vol. 274, 2021, p. 122051. <https://doi.org/10.1016/j.conbuildmat.2020.122051>.
- Yang, T., S. Chen, Y. Pan, and Y. Zhao. Investigation of the Accuracy of Fracture Energy in Evaluating the Low-Temperature Cracking Performance of Asphalt Mixture. *Journal of Materials in Civil Engineering*, Vol. 34, No. 9, 2022, p. 04022201.
- ASTM D8225-19. *Standard Test Method for Determination of Cracking Tolerance Index of Asphalt Mixture Using the Indirect Tensile Cracking Test at Intermediate Temperature*. ASTM, West Conshohocken, PA, 2019. <https://doi.org/10.1520/D8225-19>.
- AASHTO. *Standard Method of Test for Determining the Fracture Potential of Asphalt Mixtures Using Illinois Flexibility Index Test (I-FIT)*. AASHTO, Washington, D.C., 2021.
- Zofka, A., M. Maliszewski, and D. Maliszewska. Glass and Carbon Geogrid Reinforcement of Asphalt Mixtures. *Road Materials and Pavement Design*, Vol. 18, Supplement 1, 2017, pp. 471–490.
- Cullen, S., D. Offenbacher, A. Ali, Y. Mehta, C. Decarlo, and M. Elshaer. Assessing the Impact of Geosynthetic Interlayers on Laboratory Cracking and Delamination of Hot-Mix Asphalt Mixtures. *Transportation Research Record: Journal of the Transportation Research Board*, 2021. 2675: 148–160.
- American Association of State Highway and Transportation Officials. *Determining the Damage Characteristic Curve of Asphalt Concrete from Direct Tension Cyclic Fatigue Tests*. AASHTO TP 107. AASHTO, Washington, D.C., 2004.
- ASTM D7313-13. *Standard Test Method for Determining Fracture Energy of Asphalt-Aggregate Mixtures the Disk-Shaped Compact Tension Geometry*. ASTM, West Conshohocken, PA, 2013.
- American Association of State Highway and Transportation Officials. *Standard Test Method for Thermal Stress Restrained Specimen Tensile Strength*. AASHTO, Washington, D.C., 1996.
- Blankenship, P. B. Caution of Indirect Tensile Strength-Only Specifications for Asphalt Mixtures. *Blankenship Asphalt Tech and Training*, Richmond, KY, 2019.
- Liu, Z., Y. Wang, Y. Meng, Z. Han, and T. Jin. Comprehensive Performance Evaluation of Steel Fiber-Reinforced Asphalt Mixture for Induction Heating. *International Journal of Pavement Engineering*, Vol. 23, No. 11, 2022, pp. 3838–3849. <https://doi.org/10.1080/10298436.2021.1923712>.